# A well-balanced PCCU-AENO scheme for a sediment transport model

Arno Roland Ngatcha Ndengna[*,1,2] and Abdou Njifenjou[1,2,3]

*[1]Laboratory of Energy Material Modeling and Method (E3M)*
*[2]National Higher Polytechnic School of Douala, University of Douala, P.O.BOX 2701, Douala, Cameroon*
*[3]National Advanced School of Engineering, University of Yaounde I, P.O. Box: 8390, Yaounde, Cameroon*

**Abstract.** We develop in this work a new well-balanced preserving-positivity path-conservative central-upwind scheme for Saint-Venant-Exner (SVE) model. The SVE system (SVEs) under some considerations, is a nonconservative hyperbolic system of nonlinear partial differential equations. This model is widely used in coastal engineering to simulate the interaction of fluid flow with sediment beds. It is well known that SVEs requires a robust treatment of nonconservative terms. Some efficient numerical schemes have been proposed to overcome the difficulties related to these terms. However, the main drawbacks of these schemes are what follows: (i) Lack of robustness, (ii) Generation of non-physical diffusions, (iii) Presence of instabilities within numerical solutions. This collection of drawbacks weakens the efficiency of most numerical methods proposed in the literature. To overcome these drawbacks a reformulation of the central-upwind scheme for SVEs (CU-SVEs for short) in a path-conservative version is presented in this work. We first develop a finite-volume method of the first order and then extend it to the second order via the averaging essentially non oscillatory (AENO) framework. Our numerical approach is shown to be well-balanced positivity-preserving and shock-capturing. The resulting scheme could be seen as a predictor-corrector method. The accuracy and robustness of the proposed scheme are assessed through a carefully selected suite of tests.

**Keywords:** AENO reconstruction procedure; path-conservative central-upwind scheme; Saint-Venant-Exner model; sediment transport processes

## 1. Introduction

One challenge in coastal engineering is to study the dynamic of sediment in shallow water systems. Such a problem can be modeled by a set of hyperbolic nonlinear partial differential equation coupling shallow water equations (SWE) and Exner equation. SWE used in predicting surface flows is obtained by vertical integration of three-dimensional (3D) flows under shallow assumptions and the Exner model describes bed evolution or morphodynamic is derived by the mass conservation of sediment equation. The obtained well-known Saint Venant-Exner (SVE) model is a non-conservative sediment transport equation and can be solved by finite volume methods. The main difficulties with SVEs from a theoretical and numerical point of view come from the apparition of non-conservative products. For discontinuous solutions, this non-conservative product is not well-

---

∗Corresponding author, Dr., E-mail: arnongatcha@gmail.com

defined in the distributional sense. The concept of weak solution cannot be used in this case for instance. According to Dal Maso *et al.* (1995), the product can be understood as the Borel measure.

Efficiency schemes for the SVE model with topography and bottom friction source terms are required for addressing problems on the transportation sediments. Several numerical methods have been developed to solve these problems. We cite Hybrid scheme coupling Beam and warming implicit finite difference and simple finite difference by Kalita (2022), well-balanced schemes (see for instance Rosatti and Fraccarolo (2006)); Central-Upwind(CU) schemes (see Xin *et al.* 2012); Finite volume based on Riemann solver approximations and   based on Roe solver of Roe (1982) approximations (see for instance Castro *et al.* (2009), Audusse *et al.* (2015)); explicit finite volume staggered grid (see Gunawan 2015); explicit finite volume methods with stabilization Moungnutou *et al.* (2022), Njifenjou (2022a, b); splitting schemes (see for instance Siviglia *et al.* (2022), Ngatcha *et al.* (2022a)), Flux limiter methods (see for instance Benkhaldou *et al.* (2012)), Carraro *et al.* (2018) using an efficient implementation of the Dumbser-Osher-Toro (DOT) Riemann solver for 1D SVEs.

A 3D numerical model is proposed to study local scouring around single vertical piers with different cross-section shapes under steady-current flow. The model solves the flow field and sediment transport processes using a coupled approach Amir Bordbar*et al.* (2021) (see also Bakhtyar *et al.* (2016), Mohammad Barzegar and Palaniappan (2020)). Another HLL-type methods also can be used to simulate interactions between fluid flow and bottom Guozhen *et al.* (2022).

However, the main drawbacks of some above schemes are what follows: (i) Lack of robustness, (ii) Generation of non-physical diffusions, (iii) Presence of instabilities within numerical solutions. For nonconservative equations, some above schemes (as the CU based schemes) are not applicable due to presence of nonconservative product into the   SVE   model.   A   strategy   consists   to discretize this product by using a linear path according to Parès (2006). The resulting path-conservative methods are applicable for nonconservative problems. A such concept has been used by several authors, Carraro *et al.* (2018), Castro *et al.* (2009), Dumbser and Balsara (2016), Ngatcha *et al.* (2022b), Siviglia *et al.* (2022), Xin *et al.* (2015); the references therein. Path-conservative based schemes were designed to overcome these difficulties.

Note that this method has been first introduced for 1D Shallow Water and 1D two-layer Shallow Water systems. But the strategy developed in their work to preserve exactly well balanced between flux and source terms fail for the SVE model. According to the above remarks, few numerical methods for non-conservative problems designed simultaneously satisfied the following properties: well-balanced that is exactly capable to preserve steady-state solutions (lake at rest states) even in presence of wet-dry interfaces; it stably simulates the wet-dry zones without numerical oscillations; it stably handle the discontinuities since the non-conservative products are well-defined. For example, classical path-conservative methods introduced by Parès (2006) may not satisfy the balance of flux gradient and source term at the steady state in discrete level and may introduce the oscillation near the discontinuities thus the scheme becomes unstable.

The goal of this work is to develop a new high resolution first-order PCCU scheme for the non-conservative SVE model with friction source term (also called PCCU-SVEs scheme for short) exactly preserving equilibria while maintaining the positivity of the water depth. The First order PCCU scheme is extended to the second order by using a special nonlinear reconstruction technique of unknowns. Here, we suggested to use a modified AENO reconstruction technique version to eliminate nonphysical oscillations near the strong gradients or extensive numerical dissipation. This reconstruction technique is obtained by modifying the AENO procedure originally developed by Toro *et al.* (2021). AENO results in a special averaging of the ENO polynomial and its closest neighbors, while retaining the stencil direction decided by the ENO choice. The AENO-hydrostatic

reconstruction procedure is also developed in this work to handle accurate and efficient dry-wet transitions. In this paper, our primary objective is to develop a robust and highly accurate well-balanced positive PCCU-AENO scheme for a sediment transport problem.

The proposed PCCU schemes are proven to be very advantageous compared to the CU schemes also presented here and which in some situations as presented below, fail to accurately capture solutions. This is due to the presence of the non-conservative product as mentioned above. An extension to second order in time is obtained through the implementation of the third-order semi-implicit Runge-Kutta (SI-RK3) method of Chertock *et al* (2015). Another difficulty is the presence of friction source term. This term does not appear in some finite volume schemes cited above. Note that the presence of the bottom friction source term increases the level of complexity in numerical computational. Another objective is to apply SI-RK3 method to deal the friction source term. This procedure sustains the well-balanced and positivity-preserving properties of the proposed fully discrete PCCU schemes. Therefore, the new second order fully PCCU scheme developed here, consists of a predictor stage for the AENO reconstruction of discrete fluxes and correction stage for the recovery of solution.

We test the proposed PCCU schemes on various problems. The obtained results demonstrate good resolution with high accuracy in smooth regions and without any nonphysical oscillations near the steep gradients or extensive numerical dissipation. The proposed scheme can treat the discontinuities and capture shocks associated with Dam-break on erodible or non-erodible beds.

The rest of the paper is organized as follows. In Section 2, we present the coupled SVE model in different forms and we propose several properties of the system. In section 3 we present first order Central-Upwind scheme for SVE model in a version Path-conservative. In section 4, we rigorously derive the PCCU-SVE scheme for a quasi-linear form of the SVE model. In section 5, we propose a well balanced discretization topography source term and AENO well-balanced preserving-positivity reconstruction. Finally, in section 6, we present several numerical examples.

## 2. Mathematical modeling and hyperbolicity study

### 2.1 Governing equations

The model used in this work is obtained by coupling Shallow Water Equations(SWE) Barre de Saint-Venant (1871) and the well-known Exner equation Exner (1925). The Saint-Venant-Exner equations writes

$$\frac{\partial h}{\partial t} + \frac{\partial hu}{\partial x} = 0,$$

$$\frac{\partial hu}{\partial t} + \frac{\partial}{\partial x}(huu + \frac{1}{2}gh^2) = -gh\frac{\partial Z_b}{\partial x} + S_F, \tag{1}$$

$$\frac{\partial Z_b}{\partial t} + \frac{1}{(1-\lambda_p)}\frac{\partial q_b}{\partial x} = 0.$$

The system of Eqs. (1) is considered in a certain spatio-temporal domain $\Omega \times (0,T) \subset \mathbb{R} \times \mathbb{R}_+^*$. To obtain a well-posed problem we add to Eq. (1), some initial conditions and boundary conditions. In this model, $h[m]$ is the water depth, $u[m/s]$ is the vertically-averaged velocity components, $Z_b[m]$ is the bed level, $t[s]$ is the time, $x[m]$ is the streamwise coordinate and is the acceleration

gravity. The flow discharge per unit width is defined by $q = hu[m^2/s]$. The friction source term writes $S_F = -C_f |u| u$ where $C_f = gn^2(h)^{-1/3}$ is the friction factor (or the coefficient of hydraulic resistance) where $n[s/m^{1/3}]$ is the Manning's roughness coefficient. Manning's coefficient $n$ depends on the characteristic amplitude and spatial scale denoted by the irregular structure of the mobile bed $Z_b$. The Manning coefficient should be defined following a wide range of scales of bed inhomogeneities. For the small-scale inhomogeneities the amplitude $\Delta Z_b < 0.8$ we can take $n = 0.0025$. For the large-scale inhomogeneities $n$ does not exceed 0.02 Tatyana Dyakonova and Alexander Khoperskov (2018). Notice that the friction term becomes a stiff damping term, which increases the level of complexity in the development of efficient numerical methods for the Eq. (1). $q_b$ is the bedload sediment flux per unit width and $\lambda_p$ is the bed porosity. $q_b$ is given by the Grass model Grass (1981)

$$q_b = A_g * |u|^{m_g - 1} u, \quad 0 \le m_g \le 4 \tag{2}$$

where the constant $A_g(s^2/m)$ depends on experimental data and takes into account the grain diameter and the cinematic viscosity. The value is currently used, and strong interaction between fluid and sediment is simulated letting $A_g$ be close to 1. SVEs can be written in the nonconservative form

$$\frac{\partial W}{\partial t} + \frac{\partial F(W)}{\partial x} = S_{zb}(W)S(W); \quad x \in \Omega \subset \mathbb{R}, \quad t \in (0,T) \tag{3}$$

where $\dfrac{\partial F(W)}{\partial x}$ is the conservative term,

$W = \begin{pmatrix} h \\ hu \\ Z_b \end{pmatrix}$, is the vector unknowns; $F(W) = \begin{pmatrix} hu \\ hu^2 + \dfrac{1}{2}gh^2 \\ \dfrac{A_g}{(1-\lambda_p)}|u|^2 u \end{pmatrix}$, is the physical flux;

$S_{Zb}(W) = B(W)\dfrac{\partial Z_b}{\partial x}$, is the topography source term with $B(W) = \begin{pmatrix} 0 \\ -gh \\ 0 \end{pmatrix}$; and where

$S(W) = \begin{pmatrix} 0 \\ -C_f |u| u \\ 0 \end{pmatrix}$ friction source term. Using this form the SVE can be solved by a CU scheme.

Really, the SVE model is nonconservative since the derivatives $Z_b$ appear in the nonconservative product.

The nonconservative form of SVE model can be given by

$$\frac{\partial W}{\partial t} + A(W)\frac{\partial W}{\partial x} = S(W(x,t)) \quad x \in \Omega \subset \mathbb{R}, \ t \in (0,T) \tag{4}$$

In Eq. (4)

$$A(W) = \mathrm{A}(W) - \mathrm{B}(W) \tag{5}$$

$$A(W) = \frac{\partial(F(W))}{\partial W} = \begin{bmatrix} 0 & 1 & 0 \\ -u^2 + gh & 2u & 0 \\ -u\phi & \phi & 0 \end{bmatrix}, \ and \ \mathrm{B}(W) = \begin{bmatrix} 0 & 0 & 0 \\ 0 & 0 & -gh \\ 0 & 0 & 0 \end{bmatrix}.$$

$\phi = \dfrac{\partial q_b}{\partial q} = m_g.Ag\dfrac{u^{m_g-1}}{h}$, is the measure of the intensity of total bedload in flow. Here, $A(W)$ is a regular

matrix-valued function from $\Omega$ to $\mathrm{M}_{N \times N}(\mathbb{R})$. The model is hyperbolic if the Jacobian matrix $A(W)$ given by (5) as 3 distinct reals eigenvalues $\lambda_1(\mathrm{A}(W)) < \lambda_2(\mathrm{A}(W)) < \lambda_3(\mathrm{A}(W))$.

Note that the vector $\mathrm{B}(W)$, is linear in $W$ and depends only on $c = gh$. It is usual to write the nonconservative terms in terms of a matrix-vector product; but it is also possible to write it in terms of the vectors.

## 2.2 Eigenstructure of SVE model

The SVE system given byEq. (1) is strictly hyperbolic since we have three distinct real eigenvalues $\lambda_1, \lambda_2, \lambda_3$ given by

$$\lambda_1 = \frac{2}{3}u - \frac{1}{3}\Omega; \ \lambda_2 = 0, \ \lambda_3 = \frac{2}{3}u + \frac{1}{3}\Omega. \tag{6}$$

where $\Omega = \sqrt{u^2 + gh(1+\phi)}$. We have well $\lambda_1 \leq \lambda_2 \leq \lambda_3$. The three non-dimensional eigenvalues, can be analytically expressed as

$$\frac{\lambda_1}{c} = \frac{2}{3}Fr - \frac{1}{3}\Omega(Fr) \leq 0, \ \frac{\lambda_2}{c} = 0, \ \frac{\lambda_3}{c} = \frac{2}{3}Fr - \frac{1}{3}\Omega(Fr) \geq 0; \tag{7}$$

where $\Omega = \sqrt{Fr^2 - (1+\phi)}$. These eigenvalues can develop either shock or rarefaction waves Riemann invariants are constant across linearly degenerate waves and rarefaction waves, whereas for shock waves generalized jump conditions should be satisfied. The three eigenvectors corresponding to the eigenvalues $\lambda_i, \ i = 1,2,3$ are

$$R_1 = \begin{pmatrix} 1 \\ \lambda_1 \\ \dfrac{(u-\lambda_1)^2}{gh}-1 \end{pmatrix}, \ R_2 = \begin{pmatrix} 1 \\ 0 \\ \dfrac{u^2}{gh}-1 \end{pmatrix}, \ R_3 = \begin{pmatrix} 1 \\ \lambda_3 \\ \dfrac{(u-\lambda_3)^2}{gh}-1 \end{pmatrix}. \tag{8}$$

Therefore, $\nabla_W \lambda_1 . R_1 \neq 0, \ \nabla_W \lambda_2 . R_2 = 0, \ \nabla_W \lambda_3 . R_3 \neq 0.$

There is at least a genuinely non-linear field and such solutions can be constructed as simple non-linear $k - waves$. The eigenvectors are linearly independent since we have:

$\det(R_1, R_2, R_3) \neq 0.$ Hence the system is strictly hyperbolic.

### 2.3 C-property of the model

We recall that the steady states solution is satisfied by the following equation

$$\frac{\partial q}{\partial x} = 0$$
$$\frac{\partial}{\partial x}(\frac{q^2}{h} + \frac{1}{2}gh^2) = -gh\frac{\partial Z_b}{\partial x} - C_f \mid u \mid u \qquad (9)$$
$$\frac{\partial q_b}{\partial x} = 0$$

As one easily can see, the system (9) admits nontrivial $(u \neq 0)$ steady states in the form

$$q = hu \equiv constant, \ h \equiv constant, \ \frac{\partial Z_b}{\partial x} \equiv constant \qquad (10)$$

This solution corresponds to the situation when the water flows over a slanted infinitely long surface with a constant slope. It's also the situation when the fluxes of sediment are zeros. The preservation of two equilibria ensures the positivity of the water height and the well-balanced property:

-The steady states writes

$$q \equiv q_0; \ \frac{\partial Z_b}{\partial x} \equiv -K_0; \ h \equiv h_0 = \left(\frac{n^2 q_0}{K_0}\right)^{3/10}; \qquad (11)$$

The steady states "lake at rest" reads

$$u \equiv 0; \ h + Z_b \equiv const \qquad (12)$$

-the constant slope equilibrium writes

$$\partial_x h = \partial_x u = \partial_{xx} Z_b; \frac{\partial Z_b}{\partial x} + S_F = constante = 0. \qquad (13)$$

**Remark. 1**

Next, we denoted $W$ the space of steady states which satisfy Eq. (11), by $W_0$ the space which guarantees that "lake at rest" solutions are exactly preserved at discrete level and by $W_0^+$ the space which guarantees that "lake at rest" solutions are exactly preserved with the positivity of water depth at the discrete level.

**Remark. 2**

Let us remark that the validity of the well-balanced property is of great interest when erosion near a steady state is considered. For certain cases, it's needed that the projection of the Jacobian matrix of the nonconservative system onto steady states at rest space is non-singular. This is the case for SWE but not for SVEs. This can make it difficult to design a well-balanced PCCU-SVES scheme in the presence of bed sediment. A strategy of well-balanced discretization is developed here to solve this problem.

**Remark. 3**

SVEs given by Eqs. (1) and (2), arise in the modeling of sediment which occurs at very different time scales in rivers, lakes coastal estuaries. SVEs are widely used for describing the bed evolution in shallow water flows.

## 3. Well-balanced Central-Upwind scheme and reformulation

In this section, we start by presenting a CU scheme in a version path-conservative for the 1D SVE model given by Eq. (4) with uniform sediment size. We consider an open bounded domain of $\mathbb{R}$ denoted $\Omega$. The grid of $\Omega$ considered here is uniform that is $x_i = i\Delta x$, where are the small spatial scale and the corresponding finite volume cells $K_i = \left[ x_{i-1/2}, \ x_{i+1/2} \right]$. The set of all the cells is denoted $\mathbb{T}$. We have $\Omega = \bigcup_{i=1}^{N} K_i$ where $N$ is the number of cells. We denoted by $\mathbb{E}^{int}$ (respectively $\mathbb{E}^{ext}$ the set of interior edges (respectively the set of exterior edges)

$$\mathbb{E}^{ext} = \{K_i, i \in \partial\Omega\} = \{K_i, \ i \in \{1, N\}\}, \quad \mathbb{E}^{int} = \{K_i, i \in \Omega\} = \{K_i, \ i \neq 1, i \neq N\}. \tag{14}$$

We assume that at a certain time level t the solution realized in terms of its averages is available.

Integration of Eq. (4) over the cell $K_i$ provides the first order semi-discrete CU scheme for the 1-D SVE model

$$\frac{d}{dt}\bar{W}_i(t) = -\left( \frac{\mathrm{F}_{i+1/2}(t) - \mathrm{F}_{i-1/2}(t)}{\Delta x} + S(\bar{W}_i(t)) \right) \text{ in } \mathbb{E}^{int} \tag{15}$$

where the discrete source term is given by $S(\overline{W}_i(t)) = S_{zb}(\overline{W}_i(t)) + S(\overline{W}_i(t))$

The CU fluxes in Eq. (15) are given by

$$\mathrm{F}_{i+1/2} = \frac{a_{i+1/2}^+ F(W_{i+1/2}^-) - a_{i+1/2}^- F(W_{i+1/2}^+)}{a_{i+1/2}^+ - a_{i+1/2}^-} + \frac{a_{i+1/2}^+ a_{i+1/2}^-}{a_{i+1/2}^+ - a_{i+1/2}^-}\left(W_{i+1/2}^+ - W_{i+1/2}^-\right)$$

$$= \frac{a_{i+1/2}^+}{a_{i+1/2}^+ - a_{i+1/2}^-} F(W_{i+1/2}^-) - \frac{a_{i+1/2}^-}{a_{i+1/2}^+ - a_{i+1/2}^-} F(W_{i+1/2}^+) - \frac{1}{2}\left( \frac{-2a_{i+1/2}^+ a_{i+1/2}^-}{a_{i+1/2}^+ - a_{i+1/2}^-}\left(W_{i+1/2}^+ - W_{i+1/2}^-\right) \right). \tag{16}$$

We reformulate the CU numerical flux as follows

$$\mathrm{F}_{i+1/2} = \frac{1 - \alpha_1^{i+1/2}}{2} F(W_{i+1/2}^+) + \frac{1 + \alpha_1^{i+1/2}}{2} F(W_{i+1/2}^-) - \frac{\alpha_0^{i+1/2}}{2}\left(W_{i+1/2}^+ - W_{i+1/2}^-\right) \tag{17}$$

where

$$\alpha_0^{i+1/2} = \frac{-2a_{i+1/2}^+ a_{i+1/2}^-}{a_{i+1/2}^+ - a_{i+1/2}^-} \quad \text{and} \quad \alpha_1^{i+1/2} = \frac{a_{i+1/2}^+ + a_{i+1/2}^-}{a_{i+1/2}^+ - a_{i+1/2}^-} \quad \text{and where}$$

$$F(W) = \begin{pmatrix} hu \\ huu + \dfrac{1}{2}gh^2 \\ \dfrac{Ag}{(1-p)}(|u|^2 u) \end{pmatrix}.$$

Notice that all of the indexed quantities depend on $t$, but from now on we will omit this dependence for the sake of brevity. Therefore, the first order semi-discrete CU scheme writes

$$\frac{d}{dt}\bar{W}_i(t) = -\left( \frac{F_{i+1/2}(t) - (F(W_{i-1/2}^+) - F(W_{i+1/2}^-)) - F_{i-1/2}(t) + (F(W_{i-1/2}^+) - F(W_{i+1/2}^-))}{\Delta x} \right) + S(\bar{W}_i(t))$$

$$= \left( \frac{D_{i+1/2}^- + D_{i-1/2}^+ - (F(W_{i-1/2}^+) - F(W_{i+1/2}^-))}{\Delta x} \right) + S(\bar{W}_i(t)) \tag{18}$$

where $D_{i+1/2}^\pm$ are the fluctuation given by

$$D_{i+1/2}^- = F_{i+1/2} - F(W_{i+1/2}^-), \quad \text{and} \quad D_{i-1/2}^+ = -F_{i+1/2} + F(W_{i-1/2}^+). \tag{19}$$

Note that $F(W_{i-1/2}^+) - F(W_{i+1/2}^-)$ in Eq. (18) can be expressed as a function of polynomial reconstruction.

**NB.**

It possible to use the spectral decomposition to compute fluctuation since the Jacobian matrix of the system is diagonalizable.

**Remark. 4**

For conservative systems, the first-order version of the CU scheme given by Eqs. (18) and (19) coincides with the semi-discrete HLL scheme for nonconservative systems. In this semi-discrete scheme, we denoted $W_{i+1/2}^+$ *and* $W_{i+1/2}^-$ the left and right intermediate values of polynomial reconstruction

$$W(x,t) = \sum_i P_i X_{K_i}(x), \quad P_i = \left( P_i^{(1)}, P_i^{(2)}, ...., P_i^{(N)} \right)^T, \tag{20}$$

Here, $X$ is the characteristic function, $P_i^{(j)}$ are the polynomials of a certain degree satisfying the conservation and accuracy requirements defined for all $i$ by

$$\frac{1}{\Delta x}\int_{K_i} P_i(x)dx = \bar{W}_i, \text{ and } P_i^{(j)}(x) = W^{(j)}(x) + O((\Delta x)^s), \quad x \in K_i;$$

with $s$ a (formal) order of accuracy. $W(x) = (W^{(1)}, ...., W^{(N)})^t$ is the exact smooth solution. We are interested in left and right limiting values of reconstruction polynomials, often called boundary extrapolated values. The polynomial reconstruction is used to ameliorate the solution approximations at each mesh $K_i$. The order of the scheme depends on the choice of the $\mathrm{P}_i$ functions.

$$W_{i+1/2}^- = W(x_{i+1/2} - 0) = \mathrm{P}_i(x_{i+1/2}), \quad W_{i+1/2}^+ = W(x_{i+1/2} + 0) = \mathrm{P}_{i+1}(x_{i+1/2}). \tag{21}$$

$W_{i+1/2}^-$ *and* $W_{i+1/2}^+$ are connected via Riemann fan by $\gamma(W_{i+1/2}^+, W_{i+1/2}^-)$ (a curve in phase space). For some smooth $W$, we have

$$W_{i+1/2}^{\pm} = W(x_{i+1/2}) + \mathrm{O}(|K_i|^s), \quad \forall i \in \mathbb{Z} \tag{22}$$

**Proposition**

The one-sided local speeds of propagation $a_{i+1/2}^{\pm}$ are upper/lower bounds on the largest/smallest eigenvalues of Jacobian matrix given above

$$a_{i+1/2}^- = \min\left\{\frac{2}{3}u_{i+1/2}^- - \frac{1}{3}\sqrt{(u_{i+1/2}^-)^2 + 3gh_{i+1/2}^-(1 + \phi_{i+1/2}^-)}, \frac{2}{3}u_{i+1/2}^+ - \frac{1}{3}\sqrt{(u_{i+1/2}^+)^2 + 3gh_{i+1/2}^+(1 + \phi_{i+1/2}^+)}, 0\right\}$$

$$a_{i+1/2}^+ = \max\left\{\frac{2}{3}u_{i+1/2}^- + \frac{1}{3}\sqrt{(u_{i+1/2}^-)^2 + 3gh_{i+1/2}^-(1 + \phi_{i+1/2}^-)}, \frac{2}{3}u_{i+1/2}^+ + \frac{1}{3}\sqrt{(u_{i+1/2}^+)^2 + 3gh_{i+1/2}^+(1 + \phi_{i+1/2}^+)}, 0\right\}. \tag{23}$$

In this case, we have the following restriction

$$2\max(a_{i+1/2}^+, -a_{i+1/2}^-)\Delta t \leq CFL\Delta x; \quad 0 < CFL \leq 1 \tag{24}$$

where $\Delta t$ is the step time.

Note that the quantities $W_i, W_{i+1/2}^{\pm}, a_{i+1/2}^{\pm}$ depend on time, but we simplify the notation by suppressing this dependence. Note also that the conservative linear reconstruction cannot guarantee the positivity of the reconstructed point values $h_{i+1/2}^{\pm}$ even when the cell averages are positive for all $i$.

**Remark. 5**
The order of semi-discrete CU scheme Eqs. (17), (18), (20), (21) and (23) is given by order of the piecen polynomial reconstruction and the order of the ODE solver the system (18) is integrated in time.
- CU scheme can be seen as the semi-discrete version of the HLL scheme developed by Harten (1983).
- Under the condition that the reconstruction is non-oscillatory, the non-oscillatory property of the CU scheme is guaranteed. The latter is typically achieved using the AENO-based reconstruction introduced below.
- The information obtained from the local speeds of wave propagation is very capital. The information obtained from the local speeds of wave propagation is very capital.

- The semi-discrete CU scheme is well-balanced when $W_{i+1/2}^{+} - W_{i-1/2}^{-} = 0$ for all $i$ at the steady states. In this context, the invertibility of the Jacobian matrix is not required.
- CU scheme does not take into account the discontinuities of the nonconservative products at the cell interfaces.

Let's denote the approximation of the cell average value in the $i-th$ cell at the time $t = t^n$. We have the following fully discrete first order CU scheme

$$\overline{W}_i^{n+1} = \overline{W}_i^n - \frac{\Delta t}{\Delta x}\Big[ D_{i+1/2}^{-,n} + D_{i-1/2}^{+,n} - (F(W_{i-1/2}^{+,n}) - F(W_{i+1/2}^{-,n})) \Big] + S(\overline{W}_i^{n+\theta}) \qquad (25)$$

Where the reconstructed values at first order $W_{i+1/2}^{+} = W_{i+1}$, $W_{i+1/2}^{-} = W_i$ .

For $\theta = 0$, we obtain an explicit scheme and we obtain a semi-implicit scheme; however the coupling in the semi-implicit scheme is only local to the cell. The fully discrete CU scheme neglect the nonconservative term then the resulting method is only consistent with smooth solutions.

### Remark. 6

The fluctuations $D_{i+1/2}^{\pm,n}$ in Eq. (25) do not include nonconservative term $B(W)\dfrac{\partial Z_b}{\partial x}$. This term is handle directly as topography source term. Therefore the CU based schemes for SVE are not applicable. For nonconservative systems a more elegant interpretation can be given in the sense of the definition of Borel's measure. It is possible to take into account the jump contribution due to the nonconservative product into the fluctuations by using the concept of path-conservative introduced by Parès (2006).

## 4. New Path-Conservative Central-Upwind schemes

In this section, we develop a first-order PCCU scheme for the nonconservative SVE model given by Eq. (5). The second order PCCU scheme is obtained by using a modified AENO reconstruction approach.

### 4.1 First order PCCU-SVES scheme.

According to remark 6, the design of the PCCU scheme requires the choice of sufficiently smooth paths

$$\Psi_{i+1/2}(s) = (\Psi_{i+1/2}^{(1)}, \Psi_{i+1/2}^{(2)}, ...., \Psi_{i+1/2}^{(N)}, \Psi_{i+1/2}^{(N+1)}) := \Psi(s, W_{i+1/2}^{+}, W_{i+1/2}^{-}) \qquad (26)$$

connecting the two states $W_{i+1/2}^{+}, W_{i+1/2}^{-}$ across the jump discontinuity at $x = x_0$ such that a local-Lipschitz application $\Psi : [0,1] \times \Omega \times \Omega \to \Omega$ satisfies the following property

$$\Psi(0, W_{i+1/2}^{-}, W_{i+1/2}^{+}) = W_{i+1/2}^{-} \text{ and } \Psi(1, W_{i+1/2}^{-}, W_{i+1/2}^{+}) = W_{i+1/2}^{+}, \quad \forall W_{i+1/2}^{-}, W_{i+1/2}^{+} \in \Omega. \qquad (27)$$

We can define the nonconservative product as the Borel measure as in Dal Maso, Leveque, and Murrat (1989)

$$\mu_{x_0} = \left[ \int_0^1 A\left(\Psi(s, W_{i+1/2}^-, W_{i+1/2}^+)\right) \frac{d\Psi}{ds}(s, W_{i+1/2}^-, W_{i+1/2}^+) ds \right] \delta_{x_0} \tag{28}$$

where is $\delta_{x_0}$ is the Dirac function and $\mu_{x_0}$ is the fluctuation. This definition is similar to the one proposed by Volpert to define the nonconservative product. Generally, the concept of the weak solution and the definition of path-conservative schemes strongly depend on the chosen family of paths. Note that the choice of the family of paths is arbitrary. We take a particular example of the simplest linear segment path

$$\Psi_{i+1/2}(s, W_{i+1/2}^-, W_{i+1/2}^+) = W_{i+1/2}^- + s(W_{i+1/2}^+ - W_{i+1/2}^-), \quad s \in [0,1]. \tag{29}$$

However, we also can choose the nonlinear path. The generalized jump condition using the definition of paths writes:

$$\int_0^1 A\left(\Psi(s, W_{i+1/2}^-, W_{i+1/2}^+)\right) \frac{d\Psi}{ds}(s, W_{i+1/2}^-, W_{i+1/2}^+) ds = [A(W)\partial_x W]_\Psi - [B(W)\partial_x Z_b]_\Psi$$

$$= F(W_{i+1/2}^+) - F(W_{i+1/2}^-) + B(W_{i+1/2}^+, W_{i+1/2}^-)(Z_{b,i+1/2}^+ - Z_{b,i+1/2}^-) \tag{30}$$

$$= \sigma(W_{i+1/2}^+ - W_{i+1/2}^-),$$

where $\sigma$ is the speed of discontinuity propagation. The source term does not make any contribution to the jump conditions since it does not contain a derivative of $W$.

The LHS term is the fluctuation which is split right moving waves arising in the Riemann solution the fluctuation is defined by

$$G(W_{i+1/2}^+, W_{i+1/2}^-) = \int_0^1 A(\Psi) \frac{d\Psi}{ds} ds = G^-(W_{i+1/2}^+, W_{i+1/2}^-) + G^+(W_{i+1/2}^+, W_{i+1/2}^-) \tag{31}$$

where $G^-(W_{i+1/2}^+, W_{i+1/2}^-), G^+(W_{i+1/2}^+, W_{i+1/2}^-)$ are computed here by using the CU technique.

$G_{i+1/2}^-$; $G_{i+1/2}^+$ represent the differences between the numerical flux and the physical fluxes at both sides of the cell interface. We rewrite $G_{i+1/2}^\pm$ as follows

$$G_{i+1/2}^\pm = \frac{1 \pm \alpha_1^{i+1/2}}{2} \int_0^1 A(\Psi_{i+1/2}(s)) \frac{d\Psi_{i+1/2}}{ds} ds \pm \frac{\alpha_0^{i+1/2}}{2}\left(W_{i+1/2}^+ - W_{i+1/2}^-\right). \tag{32}$$

By the definition of in Eq. (5), we have

$$G_{i+1/2}^\pm = \frac{1 \pm \alpha_1^{i+1/2}}{2}\left(F(W_{i+1/2}^+) - F(W_{i+1/2}^-) - B_{\Psi,i+1/2}\right) \pm \frac{\alpha_0^{i+1/2}}{2}\left(W_{i+1/2}^+ - W_{i+1/2}^-\right), \tag{33}$$

with

$$B_{\Psi,i+1/2} = \int_0^1 B(\Psi_{i+1/2}(s, W_{i+1/2}^-, W_{i+1/2}^+)) \left(\frac{d\Psi_{i+1/2}^{(1)}}{ds}, \ldots, \frac{d\Psi_{i+1/2}^{(N)}}{ds}\right)^T ds, \tag{34}$$

where   $\Psi_{i+1/2} = \left( \Psi_{h,i+1/2}, \Psi_{hu,i+1/2}, \Psi_{Z_b,i+1/2} \right)^T$

With this new formulation of fluctuation, and using the definition of family path, we rerewrotehe CU scheme as

$$\frac{d}{dt} \overline{W}_i(t) = -\frac{1}{\Delta x} \left( G^-_{i+1/2} + G^+_{i-1/2} + \int_0^1 A(P_i(x)) \frac{dP_i}{dx} dx - B_i \right) + S_i \quad \text{in } E^{int} \tag{35}$$

Whereby the definition of linear piecewise reconstruction, we have

$$\int_0^1 A(P_i(x)) \frac{dP_i}{dx} dx = F(W^+_{i+1/2}) - F(W^-_{i+1/2}) \tag{36}$$

and where $B_i$ is discretized topography source term

$$B_i = \int_{K_i} B(P_i(x)) \left( \frac{dP_i^{(1)}}{dx}, \frac{dP_i^{(2)}}{dx}, ..., \frac{dP_i^{(N)}}{dx} \right) \quad K_i \in T \tag{37}$$

Note that a discretization of bed slope can be given by

$$B_i = \left( 0, g \frac{(h^-_{i+1/2} + h^+_{i-1/2})}{2} (Z^-_{b,i+1/2} - Z^+_{b,i-1/2}), 0 \right)^T \quad \text{in } E^{int} \bigcup E^{ext} \tag{38}$$

Since   $G^-_{i+1/2} = F(W^-_{i+1/2}) - F_{i+1/2}$,   and   $G^+_{i-1/2} = F_{i+1/2} - F(W^+_{i+1/2})$, with   $F_{i+1/2}$   defined by Eq. (17) the 1-D semi-discrete first-order PCCU scheme for SVEthe model rewritten as

$$\frac{d}{dt} \overline{W}_i(t) = -\frac{1}{\Delta x} \left( F_{i+1/2} - F_{i-1/2} - B_i - H_{\Psi,i+1/2} \right) + S(\overline{W}_i(t)), \quad \forall \, i \tag{39}$$

where we denoted the discrete nonconservative term   $H_{\Psi,i+1/2}$ by

$$H_{\Psi,i+1/2} = \frac{a^+_{i-1/2}}{a^+_{i-1/2} - a^-_{i-1/2}} B_{\Psi,i-1/2} - \frac{a^-_{i+1/2}}{a^+_{i+1/2} - a^-_{i+1/2}} B_{\Psi,i+1/2}. \tag{40}$$

with

$$B_{\Psi,i+1/2} = \left( 0, g \frac{(h^-_{i+1/2} + h^+_{i+1/2})}{2} (Z^+_{b,i+1/2} - Z^-_{b,i+1/2}), 0 \right)^T \quad \text{in } E^{int} \bigcup E^{ext} \tag{41}$$

The term   $H_{\Psi,i+1/2}$ is the contribution of   the jumps of the nonconservative products at the cell interfaces.

**Remark. 7**

The proposed PCCU scheme is seen as a version of path-conservative HLL of Dumbser and Balsara (2016) (see also Xin *et al.* (2015))

Note that this term makmakese PCCU scheme to become formally consistent with particular definition of weak solutions. Note also that this term play an important role in the robustness of the method presented here. The semi-discrete scheme can be extended to the second order by a reconstruction procedure newly developed.

**Remark. 8**

A difficulty encountered in PCCU method for sediment transport models is the need for projection of the Jacobian matrix onto the steady states space to be non-singular. This makes it possible to make the scheme well balanced in the presence of a variable sediment bed (bedforms). In case of the SWE, the Jacobian matrix of said system is non-singular which ensure the invertible and the possibility to write a discrete space of equilibrium states.

*4.2 Second order scheme: modified AENO reconstruction for PCCU-SVEs scheme*

To increase the resolution of contact waves and smooth parts of the solution, one may want to use a second-order extension of the PCCU-SVEs scheme presented above. In this subsection, we show how to design such an extension using an AENO procedure. This procedure is nonlinear and uses a piecewise polynomial reconstruction defined as follows

$$P_i(x) = \bar{W}_i + \Delta_i(x - x_i); \quad x \in K_i, \quad \text{with} \quad x_i = \frac{x_{i+1/2} - x_{i-1/2}}{2}, \tag{42}$$

where $\Delta_i = (\nabla W)_i$ are the slopes that approximate $\nabla W(x_i, t)$ in a non-oscillatory manner using a nonlinear slope obtained by convex combination of $\Delta_{i+1/2}$ and $\Delta_{i-1/2}$ as follows

$$(\nabla W)_i = \beta \Delta_{i+1/2} + (1 - \beta)\Delta_{i-1/2}, \quad \beta \in [0, 1] \tag{43}$$

where

$$\beta(r) = \frac{r}{\sqrt{\gamma^2 + r^2}} \quad \text{with} \quad r = \frac{\Delta_{i-1/2}}{\Delta_{i+1/2} + \grave{o}}, \tag{44}$$

and where

$$\Delta_{i+1/2} = \frac{\bar{W}_{i+1} - \bar{W}_i}{\Delta x}, \quad \Delta_{i-1/2} = \frac{\bar{W}_i - \bar{W}_{i-1}}{\Delta x}. \tag{45}$$

$\gamma$ is a positive parameter, $\grave{o}$ is a small positive tolerance to avoid division by zero. The result of reconstruction procedure is a non-oscillatory linear polynomial $P_i$ defined at time $t^n$ inside each $i$. This reconstruction is obtained by modifying AENO reconstruction procedure proposed by Toro *et al.* (2021) and is proven to have a formal second accuracy.

**Remark. 9**

To obtain second order PCCU-SVEs scheme, we replace the piecewise polynomial reconstruction $P_i$ in (21) by (42). Using Eq. (12), the PCCU-SVEs scheme obtained is non-well-balanced even if $W_{i+1/2}^+ - W_{i+1/2}^- = 0$. A strategy of well-balanced PCCU scheme has been developed for Saint-venant equations and for two layer Saint-Venant model with successful in Castro *et al.* (2019). This strategy is not adapted for sediment transport problems because the Jacobian matrix of system at discrete level projected in discrete space $W_0$ is not non-singular. Therefore is not invertible. Here a strategy is developed for nonconservative sediment transport problem to maintain the scheme well-balanced.

## 5. Well balanced discretization topography source term and AENO well-balanced preserving-positivity reconstruction

In this section, we propose a well balanced discretization of the topography such that $W \in \mathbb{W}_0$ by the second order PCCU-SVEs scheme. The result is used to propose AENO well-balanced preserving-positivity reconstruction.

### 5.1 Well balanced discretization topography source term

Fist, we note that the friction source term $S_f$ vanish at "lake at rest" states and therefore well balanced property of the scheme will be guarantees if the discretized cell average of geometric source term $S_i$ exactly balances the rest of numerical fluxes so that the second component of RHS of (39) vanish for the data satisfying (12). For $W \in \mathbb{W}_0$,

$$w_{i+1/2}^+ = w_{i+1/2}^- \Rightarrow h_{i+1/2}^+ + Z_{b,i+1/2}^+ = h_{i+1/2}^- + Z_{b,i+1/2}^-. \tag{46}$$

Therefore, he well balanced dicretization topography source term is given by the following relation

$$\mathrm{B}_i^{(2)} = \left(\mathrm{F}_{i+1/2}^{(2)} - \mathrm{F}_{i-1/2}^{(2)} - \mathrm{H}_{\Psi,i+1/2}^{(2)}\right) \equiv \mathrm{F}_{i+1/2}^{(2)} - \mathrm{F}_{i-1/2}^{(2)} - \frac{a_{i-1/2}^+}{a_{i-1/2}^+ - a_{i-1/2}^-}\mathrm{B}_{\Psi,i-1/2}^{(2)} + \frac{a_{i+1/2}^-}{a_{i+1/2}^+ - a_{i+1/2}^-}\mathrm{B}_{\Psi,i+1/2}^{(2)}. \tag{47}$$

where $\mathrm{F}_{i+1/2}^{(2)} = \mathrm{F}(W_{i+1/2}^+, W_{i+1/2}^+)$ is the second components of well-balanced numerical flux defined for reconstructed unknowns $W_{i+1/2}^+, W_{i+1/2}^+ \in \mathbb{W}_0$, that is

$$\mathrm{F}_{i+1/2}^{(2)} = \frac{1 - \alpha_1^{i+1/2}}{2} F^{(2)}(W_{i+1/2}^+) + \frac{1 + \alpha_1^{i+1/2}}{2} F^{(2)}(W_{i+1/2}^-), \text{ with } W_{i+1/2}^+, W_{i+1/2}^+ \in \mathbb{W}_0 \tag{48}$$

where $\mathrm{B}_i^{(2)}$ is defined above and where $\mathrm{B}_{\Psi,i+1/2}^{(2)}$ is the second component of nonconservative topography term defined according to Eq. (46) as

$$\mathrm{B}_{\Psi,i+1/2}^{(2)} = -g\left(\frac{h_{i+1/2}^+ + h_{i+1/2}^-}{2}\right)(h_{i+1/2}^+ - h_{i+1/2}^-) \tag{49}$$

The well-balanced discretization PCCU scheme is finally obtained by replacing $B_i$ given by (37) in the semi-discrete scheme given by Eq. (35) by $B_i$ given by Eqs. (47)-(49).

With this discretization procedure the proposed scheme is proven second-order well-balanced PCCU methods.

### 5.2 AENO positivity-preserving reconstruction

Here, we propose a procedure called AENO-preserving positivity reconstruction to achieve both the positivity of water depth and C-property of scheme. We introduce reconstructed values by AENO technique $h_{i+1/2}^\pm, q_{i+1/2}^\pm, Z_{b,i+1/2}^\pm$ of the unknowns to left and right of $i+1/2$. The velocity is calculated as

$$u_{i+1/2}^+ = \frac{(hu)_{i+1/2}^+}{h_{i+1/2}^+}, \quad u_{i+1/2}^- = \frac{(hu)_{i+1/2}^-}{h_{i+1/2}^-} \tag{50}$$

The right/left bed elevation at the cell interface $i+1/2$ in right is given by

$$Z_{b,i+1/2}^+ = \min(\max(Z_{b,i+1}, Z_{b,i}), w_{i+1}), \quad Z_{b,i+1/2}^- = \min(\max(Z_{b,i+1}, Z_{b,i}), w_i) \tag{51}$$

which should satisfy that

$$Z_{b,i+1/2}^\pm + h_{i+1/2}^\pm = w_{i+1/2}^\pm = const \tag{52}$$

if the still water $h_i + (Z_b)_i = const$ is given. This treatment makes the reconstructed bed elevation equal to water level at the interface of the wet cell and the dry cell. In order to preserve the reconstructed water depth nonnegative, the face values of water depth are corrected as

$$h_{i+1/2}^- = \max(0, \min(w_i - Z_{b,i+1/2}, h_i)), \quad h_{i+1/2}^+ = \max(0, \min(w_{i+1} - Z_{b,i+1/2}, h_{i+1})) \tag{53}$$

which verify at the steady states $h_{i+1/2}^+ = h_{i+1/2}^-$, and where $Z_{b,i+1/2} = \max(Z_{b,i+1/2}^-, Z_{b,i+1/2}^+)$. Finally the rest of unknowns can be recalculated as

$$u_{i+1/2}^+ = \frac{(hu)_{i+1/2}^+}{h_{i+1/2}^+}, \quad u_{i+1/2}^- = \frac{(hu)_{i+1/2}^-}{h_{i+1/2}^-}, \quad w_{i+1/2}^\pm = h_{i+1/2}^\pm + Z_{b,i+1/2}^\pm. \tag{54}$$

With this reconstruction the proposed scheme is proven positivity-preserving of the water depth.

**Remark. 10**
The above proposed strategy allows us to design a path-conservative-central upwind scheme for more situation such that in the presence of dry zones and in the presence of steady states near the bottom. The numerical scheme proposed here has been proven well-balanced and preserving-positivity.

## 6. Numerical results

Here, we assess the proposed PCCU-SVEs on a carefully selected, suite of test problems. For all the tests, the numerical stability is imposed by the Courant-Friedrich-Lewy (CFL) condition and the integration time step is evaluated by Eq. (24).
The semi-discrete path-conservative central-upwind Saint-Venant-Exner scheme is a system of time-independent ODEs that should be solved rigorously by an stable and efficient technique. We use here, third order semi-implicit Runge-Kutta (SI-RK3) time discretization based method presented in Ngatcha *et al.* (2022a). In all of the examples in the following text the gravitation constant $g = 9.81$, the porosity is $\lambda_p = 0.3$, the Manning roughness coefficient is $n = 0.028$ (since $l < 50m$ and $\Delta Z_b < 0.8$).
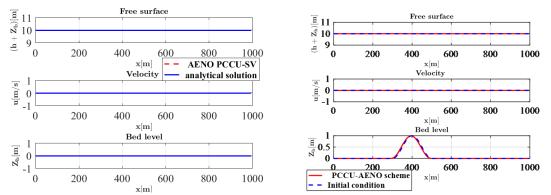
Fig. 1 C-property of PCCU-AENO method. Left for Saint-Venat model, right for Saint-Venant-Exner model
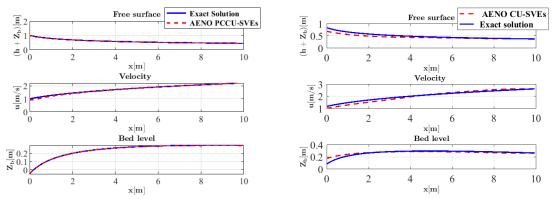


Fig. 2 High-resolution study: Comparison between the exact solution and numerical solutions obtained by both AENO CU-SVEs and AENO PCCU-SVEs schemes

Table 1 Analytical solution: high-resolution study between both CU-SVEs and PCCU-SVEs schemes

| Tests | $q_0$ | $H_0$ | $n$ | $q_b$ | $h_0$ | $\|h-h_0\|_{L^\infty}$ |
|-------|-------|-------|-----|-------|-------|------------------------|
| 1 | 0.01 | 0.01 | 0.02 | 0.6106 | 0.34 | 2.571E-16 |
| 2 | 0.01 | 0.02 | 0.02 | 0.0546 | 0.038 | 3.134E-16 |
| 3 | 0.01 | 0.015 | 0.1 | 0.0127 | 0.133 | 7.34E-16 |
| 4 | 0.01 | 0.018 | 0.1 | 6.044E-5 | 0.00735 | 1.834E-17 |
| 5 | $1/\sqrt{3}$ | 0.023 | 0.023 | 3.7904 | 0.185 | 5.67E-17 |

## 6.1 Steady states lake at rest: Verification of the C-property

We begin by illustrating the well balanced property of the designed scheme. We show that our scheme can exactly preserves the steady state solutions thus satisfying the well-balanced property. To investigate the ability of our PCCU-AENO method to preserve the correct steady-state solution, we apply the scheme to the benchmark test problem proposed in Benkhaldoun *et al*. (2012) and

Hudson (2003). Here, the domain of simulation is $\Omega = [0,\ 1000]$ and the initial conditions are defined as

$$Z_b(0,x) = \begin{cases} \sin^2(\dfrac{(x-300)\pi}{200}) & \text{if } 300 \le x \le 500, \\ 0 & \text{else} \end{cases} \quad h(0,x) = 10 - Z_b(0,x), \quad u(x,0) = 0. \quad (55)$$

The computational parameters are : $CFL = 0.1$, AENO reconstruction is performed using $TOL = 0.0001$, $\grave{o} = 1$.

The results of the simulation are presented in Fig. 1.

It is expected that the water free surface remains constant and the water velocity should be zero at all times. \We run the PCCU-AENO method using 200 gridpoints and the obtained results are displayed at a time $t = 20000\ sec$. In Table 1, we present the water free-surface and the errors in the water free-surface for the SVE model. As can be seen, the water free surface remains constant during the simulation times and the proposed PCCU-AENO method preserves the C-property to the machine precision. The computed and analytical water free surfaces are virtually indistinguishable from the SVE systems of equations. An important point presented in Fig. 1 is that our proposed scheme can identify the behavior of the numerical scheme when the sediment transport vanishes since we recovered a relevant scheme for the classical SW model.

We consider here an accuracy test where the smooth analytical solution exists. This solution refers to a steady-state condition for a subcritical water flow coupled with a linear-in-time bed erosion, as proposed by Berton. In this simulation, we let the friction term vanish $S(W) = 0$. The error between the numerical solutions and the reference solution is computed and the convergence rate is deduced. the error is evaluated in $L^p norm$ at the time $t = 7s$.

### 6.2 Accuracy test: comparison with exact solutions

Here we verify the accuracy of our numerical method by studying empirical convergence rates using the nonlinear least squares. In this application, we use both AENO CU-SVEs and AENO PCCU-SVEs schemes to approximate the Saint-Venant-Exner model presented above in domain which are approximately second order in space and time and using the original nonlinear reconstruction technique presented here. The computational domain is discretized by a mesh point. The exact solution is given by Berton *et al.* (2012)

$$q_{anal} = 1$$

$$u_{anal}(x) = \left[ \frac{\alpha x + \beta}{Ag} \right]^{1/3}$$

$$h_{anal}(x) = \frac{q_{anal}}{u_{anal}} \quad (56)$$

$$Z_{b,anal} = 1 - \frac{u_{anal}^3 + 2gq_{anal}(x)^2}{2gu_{anal}}$$

where $A_g = \alpha = \beta = 0.005$.

Table 2 Estimate error between the exact solution and numerical solution obtained by using the proposed AENO PCCU-SVEs scheme. AENO reconstruction is performed with $\grave{o} = 0.0001, \gamma = 1, CFL = 0.5$.

| | $h$ | | $u$ | | $Z_b$ | |
|---|---|---|---|---|---|---|
| $N$ | $L^\infty$ | $O(L^\infty)$ | $L^\infty$ | $O(L^\infty)$ | $L^\infty$ | $O(L^\infty)$ |
| 50 | 3.38E-2 | / | 9.8E-2 | / | 3.5E-2 | / |
| 100 | 1.95E-2 | 0.805 | 6.67E-2 | 0.55 | 1.95E-2 | 0.84 |
| 200 | 1.08E-2 | 0.903 | 4.58E-2 | 0.54 | 1.03E-2 | 0.92 |
| 400 | 5.71E-3 | 0.95 | 2.81E-2 | 0.704 | 5.33E-3 | 0.9504 |
| 800 | 2.96E-3 | 0.7507 | 1.59E-2 | 0.821 | 2.71E-3 | 0.97 |
| 1600 | 1.51E-3 | 0.984 | 8.48E-3 | 0.906 | 1.37E-3 | 0.984 |

Table 3 Estimate error between the exact solution and numerical solution obtained by using the proposed AENO PCCU-SVEs scheme. AENO reconstruction is performed with $\grave{o} = 0.0001, \gamma = 1, CFL = 0.5$.

| | $h$ | | $u$ | | $Z_b$ | |
|---|---|---|---|---|---|---|
| $N$ | $L^1$ | $O(L^1)$ | $L^1$ | $O(L^1)$ | $L^1$ | $O(L^1)$ |
| 50 | 1.16E-2 | / | 2.74E-2 | / | 6.54E-3. | / |
| 100 | 3.59E-3 | 1.69 | 1.029E-2 | 1.425 | 2.29E-3 | 1.28 |
| 200 | 1.09E-3 | 1.81 | 3.38E-3 | 1.59 | 1.13E-3 | 1.25 |
| 400 | 3.29E-4 | 1.72 | 1.03E-3 | 1.714 | 5.02E-4 | 1.17 |
| 800 | 9.49E-5 | 1.79 | 2.92E-4 | 1.81 | 2.32E-4 | 1.11 |
| 1600 | 2.6E-5 | 1.84 | 7.86E-5 | 1.89 | 1.11E-4 | 1.06 |
| 3200 | 6.87E-6 | 1.901 | 2.05E-5 | 1.93 | 5.43E-5 | 1.03 |

The comparison is made for both analytical and numerical solutions obtained by both CU-SVEs and PCCU-SVEs schemes. Results displayed in Fig. 2, demonstrate that the proposed scheme describes the bed level and water height evolution with good accuracy. We can see that the analytical solution is well approximated by both schemes. We can see that both numerical solutions converge to the analytical one.

We can see that the analytical solution is well approximated by both schemes. We can see that both numerical solutions converge to the analytical one. We can also see that both schemes converge to the same solution, but the convergence of the AENO PCCU-SVEs scheme is much faster, which confirms the high resolution and robustness of the proposed AENO PCCU-SVEs approach.

Here, we also compute first and second-order PCCU schemes. Table 2 shows the discrete where $p = 1, \infty$ of the error for $h, q$ and $Z_b$ in the first order and second order respectively at the final time step $t = 7$. We can see clearly that the second order AENO PCCU-SVEs proposed in this work have a good convergence rate $O(L^1)$ in various grid numbers where it tends to 2 for the AENO PCCU-SVEs scheme and to 1 for first order PCCU-SVEs scheme. The convergence rate of discrete $L^1 - norm$ in and $Z_b$ are shown nicely increasing along with the increasing number of points.
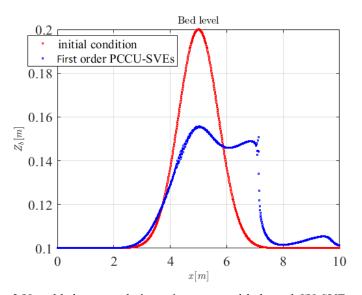
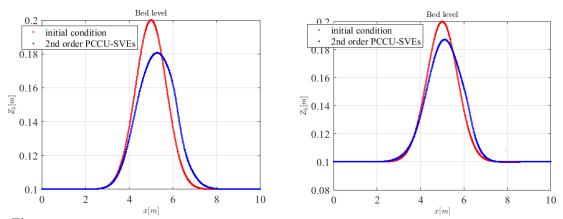Fig. 3 Unstable bump evolution using non-weel-balanced CU-SVEs scheme



Fig. 4 Bump evolution Ag=0.009, the CFL condition is 1. Left without friction source term, right with friction source term; ANEO-type reconstruction is performed using $Ò = 0.0001$ and $\gamma = 1$.

## 6.3 Short term propagation of a small sediment hump

Here, we reproduced bed movement under shallow water flow. The initial conditions are obtained by running equation following

$$Z_b(0, x) = 0.1 + 0.1 \exp(-(x-5)^2), \quad h(0, x) = 0.4 - Z_b(0, x), \quad q(0, x) = 0.6. \qquad (57)$$

We first use the non-well-balanced scheme which is the scheme without AENO-preserving positivity reconstruction proposed in subsection *5.1*. The non-well balanced discretization uses the bottom discretization given by Eq. (28). The solution using that is displayed in Fig. 3.
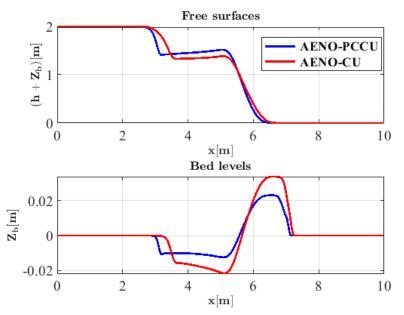
Fig. 5 Dam break over dry bed. Sediment transport is inhibited setting Ag=0.005, in Grass formula. The computational parameters are: N=200, Tfinal=1s, CFL = 0.9, AENO reconstruction is performed using $\grave{o} = 0.0001$ and $\gamma = 1$.

The Fig. 3 show that non-use of the AENO well-balanced preserving-positivity reconstruction into the CU scheme can produce unphysical and oscillatory bed profile. As one can clearly see, even under a weak-energetic flow considered in this example, the non-well balanced discretization cannot predict a stable bed erosion process. Our AENO reconstruction allows us to be agreement with the physics of the problem studied. The well-balanced solutions obtained by this reconstruction is plotted and presented in Fig. 4.

Fig. 4 shows the evolution of a sediment bump due to the mean current velocity. The bump moved upward with water flow and reduced its height. Especially in the front of the bump, the gradient of sediment discharge is positive due to the increase in flow velocity and this causes bed erosion that is $\frac{\vec{q}}{q} \cdot \frac{\nabla q}{q} > 0$. Conversely deposited on the back of the dune where the gradient of sediment discharge is negative i.e., $\frac{\vec{q}}{q} \cdot \frac{\nabla q}{q} < 0$. The variation of discharge is due to the redistribution of flows around sedimentary forms in the direction of flow. This variation coupled to advection has strong effect on the evolution of the bump on one hand by moving it in the flow and on other hand by modifying its geometry. The numerical results presented in Fig. 4, demonstrate that the proposed scheme describes the bump evolution with good accuracy, similtorom those obtained by Putu (2015).

### 6.4 Erodible dam break tests

### 6.4.1 Comparison between CU-AENO scheme and PCCU-AENO scheme
Similar tests have been presented in Wu (2005) and reproduced in Audusse *et al.* (2016). Few
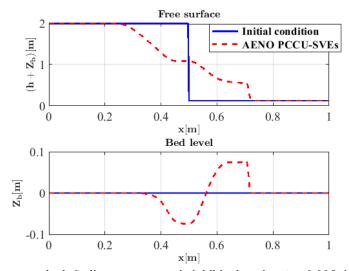
Fig. 6 Dam break over wet bed. Sediment transport is inhibited setting Ag=0.005, in Grass formula. The computational parameters are: N=200, Tfinal=1s, CFL = 0.9, AENO reconstruction is performed using $\grave{o} = 0.0001$ and $\gamma = 1$.

work reproduced with accuracy this problem with very small water depth. One are not adapted to handle vaccum at least in the way we computed them. The sediment load is $Z_b(0,x) = 0,$ fluid velocity $u(0,x) = 0$ and friction term is introduced, the final time is $t = 1$. The domains of simulation are $\Omega = [0,10]$ and $\Omega = [0,1]$ with a dam located at the middle of $\Omega$. For a first test, The dam separates two initial water depth exhibits wet zone are $h(0,x) = 2m$ at the left side and at $h(0,x) = 0.125m$ or the right side of the domain. The both AENO CU-SVEs and AENO PCCU-SVEs schemes are computed and plotted in Fig. 6. For the second test, the dam separates by $h(0,x) = 2m$ at the left side and $h(0,x) = 10^{-10} m$ (very small water depth) at for the right side of the domain. Both CU and PCCU schemes are computed and plotted in Fig. 5.

The results (Fig. 6) of dam break on wet bed problem are agreement with results given by using a Riemann solver presented in Audusse *et al*. (2015) . The non-entropic character is not observed in rarefaction wave zone by the simulations. The scheme shows very well the evolution of movable bed. It observe that, both AENO PCCU and AENO CU solutions exhibit quite similar behavior at small times. At larger times, however, the two schemes begin to produce very different results. The numerical simulations show that the AENO PCCU-SVEs scheme is able to treat accurately dry-wet transitions.

### 6.4.2 Dam break test with different grain sizes

Ones compare in this test different profiles of free surfaces, bed levels and velocities using our PCCU-AENO scheme and different sediment diameters $d_1 = 0.001, d_2 = 0.08, d_3 = 0.01, d_4 = 0.1$. The sediment load is $Z_b(0,x) = 0,$ fluid velocity $u(0,x) = 0$ and friction term is introduced, the final time is $t = 1$. The domains of simulation are $\Omega = [0,8]$ with a dam located at the middle. The water depth is given as in first case above (wet zones). The results are plotted in Fig. 7. The test
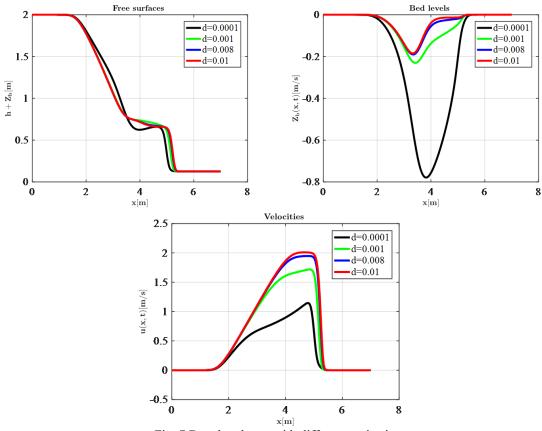
Fig. 7 Dam break test with different grain sizes

shows that the proposed numerical modeling is able to simulate a wide range of sediment class size.

We expected that the performance of our scheme can depend on sediment diameter. This is due to the Exner model. In fact, this classical model uses some empiric formulas which gives approximate results only on a certain flow regime and sediment diameter. Certain of these formulas become uncertain when the sediment diameter become greater.

### 6.5 1D Riemann problem

We consider here a similar the test case used in Bhole *et al.* (2019). Its a Riemann problem where initially

$$u = 0, \ Z_b = 0, \ \begin{cases} h = 0.02 \ \text{if} \ x < 5, \\ h = 0.01 \ \text{if} \ x > 5. \end{cases} \tag{58}$$

For this Riemann data, we can compute the associated analytical solution (but is not plotted here). Numerical approximations is performed with AENO PCCU-SVEs and AENO CU-SVEs. The results are displayed and presented in Fig. 7.
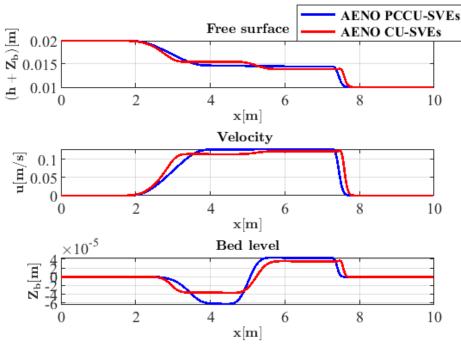
Fig. 8 Dam break computed using the PCCU-SVEs and CU-SVEs schemes with 200 cells and second order approximations. The computational parameters are: N=200, CFL = 0.5, AENO reconstruction is performed using $\grave{o} = 0.0001$ and $\gamma = 1$.

It observed that, both AENO PCCU-SVEs and AENO CU-SVEs solutions exhibit quite similar behavior at the first moment of the break. During the time, however, the two schemes begin to produce very different results. The AENO CU-SVEs solution begins to develop small perturbation after a certain moment and will eventually become unstable. This is not the case for the AENO PCCU-SVEs solution which remains stable at all time simulation. This is another strong evidence of the robustness of the proposed AENO PCCU-SVEs scheme.

## 7. Conclusions

In this paper, a new numerical method has been developed to solve a sediment transport problem by means path conservative central-upwind technique coupled with a AENO based methodology. The model studied here consists of a coupling of hydrodynamical component that is modeled by a 1D shallow-water system and a bed evolution model given by Exner equation. A strategy of well-balnaced discretization has been proposed to maintain equilibria. AENO-hydrostatic reconstruction has been proposed to maintain the positivity of the water depth. SI-RK3 method has been implemented to achieve the second order of accuracy in space and time.

After a careful study of the resulting the systems of PDEs, we proposed a methodology for their numerical solution in the framework of Godunov-type method. Finally we assess the robustness of our scheme considering different test cases. Results demonstrate that the solution converge correctly to second order of accuracy in space and time, satisfies the well-balanced property and preserves the

positivity of water depth. We have seen that AENO PCCU scheme gave better results than the original CU scheme. The numerical tests show also that our nonlinear slope limiter is very interesting and is able to eliminate of oscillations near the discontinuities. The developed scheme has good performance and can solve several sediment transport problems well. Future work is extended to study the numerical solutions of the two-dimensional case.

## Conflict of interests

The authors declare that there is no conflict of interests regarding the publication of this paper.

## Acknowledgements

## References

Audusse, E., Bouchut, F., Bristeau, M.O., Klein, R. and Perthame, B.(2004), "A fast and stable well-balanced scheme with hydrostatic reconstruction for shallow water flows", *SIAM J. Sci. Comput.*, **25**(6), 2050-2065. https://doi.org/10.1137/S1064827503431090.

Audusse, E., Ung, P. and Challons, P. (2015), "A simple three-wave approximate riemann solver for the saint-venant-exner equations", *Commun. Math. Sci.*, **13**(5), 1317-1332.

Bakhtyar, R. Dastgheib, A., Roelvink, D. and Barry D.A. (2016), "Impacts of wave and tidal forcing on 3D nearshore processes on natural beaches. Part II: Sediment Transport", *Ocean Syst. Eng.*, **6**(1), 61-97. https://doi.org/10.12989/ose.2016.6.1.023

Barré de Saint-Venant, A.J.C. (1871), "Théorie du mouvement non-permanent des eaux, avec application aux crues des rivi`ere et `a l'introduction des mar´ees dans leur lit", *Comptes Rendus de L'Acad´emie des Sciences*, **73**, 147-154.

Barzegar, M. and Palaniappan, D. (2020),"Numerical study on the performance of semicircular and rectangular submerged breakwaters", *Ocean Syst. Eng.*, **10**(2), 201-226. https://doi.org/10.12989/ose.2020.10.2.201.

Benkhaldoun, F., Sari, S. and Seaid, M. (2012), "A flux-limiter method for dam-break flows over erodible sediment beds", *Appl. Math. Model.*, **36**(10), 4847-4861. https://doi.org/10.1016/j.apm.2011.11.088.

Berthon, C., Cordier, S., Delestre, O. and Le, M.H. (2012), "An analytical solution of the Shallow Water system coupled to the Exner equation", *Comptes Rendus Mathematique*, **350**(3-4), 183-186. https://doi.org/10.1016/j.crma.2012.01.007.

Bhole, A., Nkonga, B., Gavrilyuk, S. and Ivanova, K. (2019), "Fluctuation splitting Riemann solver for a non-conservative modeling of shear shallow water flow", *J. Comput. Phys.*, **392**, 205-226. https://doi.org/10.1016/j.jcp.2019.04.033.

Bordbar, A., Sharifi, S. and Hemida, H. (2021), "Prediction of scour around single vertical piers with different cross-section shapes", *Ocean Syst. Eng.*, **11**(1), 43-58. https://doi.org/10.12989/ose.2021.11.1.043.

Carraro, F., Valiani, A. and Caleffi, V. (2018), "Efficient analytical implementation of the DOT Riemann solver for the de Saint Venant-Exner morphodynamic model", *Adv. Water Resour.*, **113**, 189-201. https://doi.org/10.1016/j.advwatres.2018.01.011.

Chertock. A., Cui, S., Kurganov, A. and Wu, T. (2015), "Steady state and system preserving semiimplicit Runge-Kutta methods for ODEs with stiff damping term", *Int. J. Numer. Meth Fl.*, **78**, 355-383.

Dal Maso, G., Lefloch, P.G. and Murat, F. (1995), "Definition and weak stability of nonconservative products",

*J. Math. Pures Appl.*, **74**(6), 483-548.

Diaz, M.J.C., Fernandez Nieto, E.D. and Ferreiro, A.M. (2009), "High order extension of Roe schemes for two dimensioal non conservative hyperbolic systems", *J. Sci. Comput.*, **39**, 67-114. https://doi.org/10.1007/s10915-008-9250-4.

Díaz, M.J.C., Kurganov, A. and Luna, T.M. de (2019), "Path conservative central-upwind for non conservative hyperbolic systems", *ESAIM: M2AN*, **53**(3), 959-985. https://doi.org/10.1051/m2an/2018077.

Dumbser, M. and Balsara, D.S. (2016), "A new efficient formulation of the HLLEM riemann solver for general conservative and non-conservative hyperbolic systems", *J. Comput. Phys.*, **304**, 275-319.

Dyakonova T. and Khoperskov, A. (2018), "Bottom friction models for shallow water equations: Manning's roughness coefficient and small-scale bottom heregeneity", *J. Phys. Conference series*, **973**(1), 012032, https://doi.org/10.1088/1742-6596/973/1/012032.

Exner, F.M.(1925), "Uber die Wechselwirkung zwischen Wasser und Geschiebe in Fl ussen", *Akademie der Wissenschaften*, *Sitzungsberichte*, **134**, Wien, Austria.

Gottlieb,S., Shu, C.W. and Tadmor, E. (2001), "Strong stability preserving high order time discretization methods", *Siam Rev.*, **43**(1). https://doi.org/10.1137/S003614450036757X.

Grass, A.J. (1981), "Sediment transport by waves and currents", Department of civil engineering, University college, London.

Gunawan, H.P. (2015), "Numerical simulation of shallow water equations and related models", General Mathematics [math.GM], Universit´e Paris-Est. English. NNT : 2015PEST1010ff. tel-01216642v2ff.

Guozhen, C., Luo, M., Zhaoheng, W. and Khayyer, A. (2022), " SPH simulation of wave interaction with coastal structures", *Ocean Syst. Eng.*, **12**(3), 285-300. https://doi.org/10.12989/ose.2022.12.3.285.

Harten, A., Lax P. and van Leer, B. (1982), "Upstream differencing and Godunov-type scheme for hyperbolic conservation laws, Upwind and High-Resolution Schemes", 53-79, https://doi.org/10.1007/978-3- 642-60543-74.

Hudson, J. and Sweby, P.K. (2003), "Formations for numerically approximating hyperbolic systems governing sediment transport", *J. Sci. Comput.*, **19**, 225-252. https://doi.org/10.1023/A:1025304008907.

Kalita H.M. (2022), "An efficient 1D hybrid numerical model for bed morphology calculations in Alluvial Channels", *Iran J. Sci. Technol. Trans. Civ Eng.*, https://doi.org/10.1007/s40996-022-00977-9.

Kurganov, A. (2018), "Finite volume schemes for shallow-water equations", **27**, *Acta Numerica*, 289-351. https://doi.org/10.1017/S0962492918000028.

Kurganov, A. and Tadmor, E. (2000), "New high-resolution central-schemes for nonlinear conservation laws and convection-diffusion equations", *J. Comput. Phys.*, **160**(1), 241-282. https://doi.org/10.1006/jcph.2000.6459.

Liu, X., Mohammadian, A. and Infante Sedano, J.A. (2012), "One dimensional numerical simulation of bed changes in irrigation channels using finite volume method", *Irrigat Drainage Sys. Eng.*, **1**, 103. https://doi.org/10.4172/2168-9768.1000103.

Liu, X., Mohammadian, A., Kurganov, A and Infante Sedano, J.A. (2015), "Well-balanced central-upwind scheme for a fully coupled shallow water system modeling flows over erodible bed", *J. Comput. Phys.*, **300**, 202-218.

Moungnutu, I., Ngtacha, A. and Njifenjou, A. (2022), "Stabilization of a finite solution for 1D Shallow Water problems", Preprint ResearchGate, October 2022, https://doi.org/10.13140/RG.2.2. 32013.82403.

Ngatcha, A., Nkonga, B. and Njifenjou, A. (2022a), "Finite volume AENO methods with flux time-steps discretization procedure for a averaged sediment transport model", In 2022. hal-03668098.

Ngatcha, A., Nkonga, B., Njifenjou, A. and Onguene, R. (2022b), "Sediment transport models in Generalized shear shallow water flow equations", Colloque Africain sur la recherché en informatiqe et en mathematiques appliquées, Oct 2022, Dschang, Cameroon. <hal-03735893>.

Njifenjou, A. (2022a), "Overview on conventional finite volumes for elliptic problems involving discontinuous diffusion coefficients. Part 1: Focus on the one dimension space models", ResearchGate, https://doi.org/10.13140/RG.2.2. 27472.17925.

Njifenjou, A. (2022b), "Geometric arguments for proving the discrete maximum principle met by conventional finite volume schemes in the context of isotropic diffusion problems", ResearchGate,

https://doi.org/10.13140/RG.2.2.16845.5168.

Parés, C. (2006), "Numerical methods for nonconservative hyperbolic systems: A theoretical framework", *SIAM J. Numer. Anal.*, **44**, 300-321.

Roe, P.L. (1986), "Upwinding difference schemes for hyperbolic conservation Laws with source terms", In Carasso, Raviart and Serre, editors, proceeding the conference on hyperbolic problems, 41-51.

Rosatti, G. and Fraccarolo, L. (2006), "A well-balanced approach for flows over mobile-bed with high sediment transport", *J. Comput. Phys.*, **220**(1), 312-338. https://doi.org/10.1016/j.jcp.2006.05.012.

Siviglia, A., Vanzo, D. and Toro, E.F. (2021), "A splitting scheme for the coupled Saint-Venant-Exner model", *Adv. Water Resour.*, **159**, 104062. https://doi.org/10.1016/j.advwatres.2021.104062.

Toro, E.F., Santaca, A., Montecinos, G.I., Muller, L.O. (2021), "AENO: a novel reconstruction method in conjunction with ADER schemes for hyperbolic equations", *Commun. Appl. Math. Comput.*, https://doi.org/10.1007/s42967-021-00147-0.

Volpert, A.I. (1967), The spaces BV and quasilinear equations, Mathematics of the USSR-Sbornik,2 (1967), 225-267.

Wu, W. and Wang, S.S. (2007), "One-dimensional modelling of dam-break flow over movable beds", *J. Hydraulic Eng.*, **133**, 48-58.


*MK*